Research on Chaos Dynamic Characteristics of Hybrid Squeeze Film Damper with Electro-hydraulic Active Control

Yunhua Li[1]
School of Automation Science and Electrical Engineering
Beijing University of Aeronautics and Astronautics
Beijing, China
1: yhli@buaa.edu.cn

Chieh-Li Chen[2]
Institute of Aeronautics and Astronautics
National ChengKung University
Tainan 701, Taiwan
2: chiehli@mail.ncku.edu.tw

***Abstract*—In this paper, addressed to the problems existed in the squeeze film damper (SFD) based on the dynamic pressure bearing in the rotational machinery, a new type of the hybrid squeeze film damper (HSFD) with piezoelectric crystal electro-hydraulic active control is proposed. It is composed of dynamic pressure bearing and static pressure bearing. The effectiveness of HSFD is analyzed theoretically, and the simulation of the chaos dynamics characteristics is carried out. The results obviously show that the HSFD not only overcomes the bi-stable problem, but also restrains the shock in the rotor supporting system.**

***Keywords*—rotor dynamics, dampers, nonliner dynamics, active control, hydraulic control**

I. INTRODUCTION

SFD is an important component of damper in the rotor supporting system and has a good damping effect to restrain not a large amount of the unbalanced force. However, as a result of highly nonlinear in the change of oil film force adapting to the bearing eccentricity, the nonlinear dynamic actions such as bi-stable state, bifurcation and chaos will appear and have an impact on the work of aero-engine. Research on nonlinear dynamic activity and active control of bearing-rotor supporting system has become a focus in several cross-disciplinary fields which are among rotor dynamics, vibration and control.

The representative studies of bearing-rotor dynamics and control are focused on the following aspects: 1) Nonlinear behavior analysis of SFD bearing-rotor system. Cooper firstly observed the phenomenon of the bi-stable state from experimental and analyzed the effect on the bi-stable state from the Jeffcott's bearing-rotor system design parameters[1,5]; Meng and Xue analyzed the bi-stable state of SFD flexible bearing-rotor system with the retaining spring, and indicated that the nonlinear response of system presents as the Duffing's nonlinearity, additional branch nonlinearity and the combination of the former and the latter[1,5]; Zhao and Hahn researched on the bifurcation and chaos dynamic characteristics of nonlinear SFD flexible bearing-rotor system by using shaft-centre-locus, Poincare's map and bifurcation diagram[8]. 2) Passivity damping device composed of the other type of dampers and SFD can restrain the SFD nonlinear affection and it can improve damping effects [4,10]. For example, Zhang and Yan proposed PSFD by combining power metallurgical ring and SFD, and supported the external ring using a metal rubber ring. 3) The vibration active control theory of the SFD and its implementation [1,5,4,10]. The implement methods of active control mainly contain auxiliary electromagnetic bearing method, alternating retaining-spring stiffness method, piezoelectric actuator controlling centering spring stiffness method, ER fluid supporting method and controllable hybrid bearing, etc. Among of them, the last one is most likely to be practically used as an active damping device on account of a few changes on SFD, small additional mass and good controllability.

HSFD to be introduced in this study uses static pressure bearing to improve the dynamic characteristics of the SFD. As shown in Fig.1, it has 4 static pressure area, axial dynamic pressure area and rotational pressure area. By changing the pressure in the static pressure range, the controllability of HSFD can be achieved.

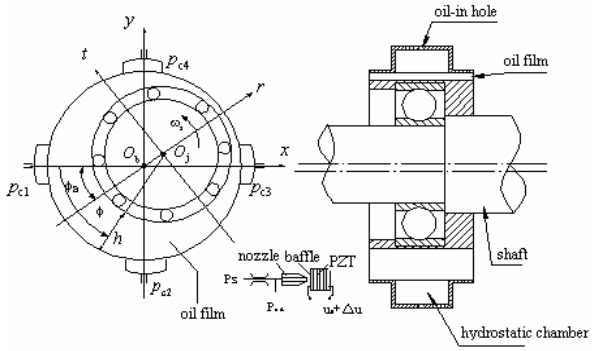

Figure 1. HSFD system working principle

The paper is arranged as follows. Section 2 establishes a mathematical model of HSFD system, researches the nonlinear behavior of the HSFD on that basis for researching on the chaos dynamic characteristics of SFD, and calculates various

Project 59975003 supported by National Natural Science Foundation of China and project NSC89-2212-E006-097 supported by National Science Council of Taiwan.

indexes of the rotor-supporting system, such as phase trajectory, power spectrum, the Poincare's mapping, and the overall bifurcation diagram. Section 3 discusses the appropriate control strategy to eliminate cycle times and chaotic motion based on the research results, so the active control on the bearing-rotor can be achieved. Finally, the conclusions and recommendations for further work are given.

II. MATHEMATICAL MODELING OF HSFD SYSTEM

Fig.1 is a principle diagram of HSFD and the rotor. It consists of a controllable hybrid bearing, a hydraulic half-bridge driven by piezoelectric actuator, a controller and a power supply. The rigid rotor is supported on the device by a roller bearing with HSFD and a retaining spring. A controllable damping force can be formed to achieve active damping by the squeeze-film damper. It divides the regular oil chamber into four independent static pressure regions at rotational direction. For the sake of convenience, the following assumptions of HSFD are made as

A1: The oil in HSFD is incompressible fluid with the same viscosity;

A2: The fluid between axis and dynamic pressure region is laminar flow;

A3: The depth of oil chamber is much larger than the clearance of damper and the pressure in the oil chamber is considered to be a constant;

A4: The elastic deformation between the bearing and the bearing housing is negligible and flow inertia is negligible;

A5: The configuration of HSFD is symmetric and the size of each oil chamber is identical.

A. Pressure distribution equations

Based on the assumption of incompressible and oil film bearing theory in the reference [4], the Reynolds equation is given as follows

$$\frac{1}{R^2}\frac{\partial}{\partial\theta}(h^3\frac{\partial p}{\partial\theta})+\frac{\partial}{\partial z}(h^3\frac{\partial p}{\partial z})=12\mu(\dot{\varepsilon}\cos\theta+\varepsilon\dot{\phi}_B\sin\theta)C \qquad (1)$$

where R represents radius of oil film. $\theta=\phi-\phi_B$, $\varepsilon=e/C$ mean dimensionless eccentricity, C means clearance of radius, ϕ_B means the motion angle of bearing axis, μ means dynamic viscosity of lubricating oil, and p represents the pressure of oil film.

The pressure distribution of HSFD can be divided into 3 parts: static pressure region, rotation direction dynamic pressure region and axial direction dynamic pressure region. The pressure inside the static pressure range is constant. Each pressure $p_{c,i}$ of the four ranges is as follows:

$$\begin{cases} p_{c,1}=p_s-\Delta p_1, p_{c,2}=p_s-\Delta p_2 \\ p_{c,3}=p_s+\Delta p_1, p_{c,4}=p_s+\Delta p_2 \end{cases} \qquad (2)$$

where p_S represents the pressure of oil supply. The differential pressure Δp_1 of range 1 and 3 and the differential pressure Δp_2 of range 2 and 4 are decided by the following equations. k_p and k_d respectively on behalf of proportion and differential coefficients.

$$\begin{cases} \Delta p_1=k_p x+k_d\dot{x} \\ \Delta p_2=k_p y+k_d\dot{y} \end{cases} \qquad (3)$$

In the polar system, Eq.(3) can be transformed as follows

$$\begin{cases} \Delta p_1=k_p\varepsilon\cos\phi_B+k_d(\dot{\varepsilon}\cos\phi_B-\varepsilon\dot{\phi}_B\sin\phi_B) \\ \Delta p_2=k_p\varepsilon\sin\phi_B+k_d(+\dot{\varepsilon}\sin\phi_B+\varepsilon\dot{\phi}_B\cos\phi_B) \end{cases} \qquad (4)$$

The pressure distributing of dynamic pressure range and axis can be decided based on solving Reynolds equations (1) after deciding each range's pressure as the boundary conditions.

In the area $-a\le z\le a$ of the HSFD, the pressure in the static pressure region is constant as $p_{c,i}$ and the pressure in the dynamic pressure region can be solved by using the long bearing theory. In the area $a\le|z|\le L/2$ of the HSFD, the pressure can be solved by using short bearing theory and the boundary condition of $p(z,\theta)\big|_{z=\pm a}=p_0(\theta)$ and $p(z,\theta)\big|_{z=\pm L/2}=0$. The pressure distribution is shown in Fig.2 and Fig.3. and $p_0(\theta)$ can be written as

$$p_0(\theta)=\begin{cases} p_{c,i} & \frac{\pi}{2}(i-1)-\frac{\beta}{2}-\phi_B\le\theta\le\frac{\pi}{2}(i-1)+\frac{\beta}{2}-\phi_B \\ p_i(\theta) & \frac{\pi}{2}(i-1)+\frac{\beta}{2}-\phi_B\le\theta\le\frac{\pi}{2}i-\frac{\beta}{2}-\phi_B \end{cases} \qquad (5)$$

According the pressure distribution assumed in Fig.3, solve the Eq.(1), we can get the pressure distribution $p_i(\theta)$ as follows

$$p_i(\theta)=p_{c,i}+\frac{6\mu R^2}{C^2}\frac{\dot{\varepsilon}}{\varepsilon}\left[\frac{1}{(1+\varepsilon\cos\theta)^2}-\frac{1}{(1+\varepsilon\cos\theta_{i1})^2}\right]+ C_1\int_{\theta_{i1}}^{\theta}\frac{1}{C^3(1+\varepsilon\cos\theta)^3}d\theta-\int_{\theta_{i2}}^{\theta}\frac{12\phi_B\mu C\varepsilon R^2\cos\theta}{C^3(1+\varepsilon\cos\theta)^3}d\theta \qquad (6)$$

where $i=1,2,3,4$, $\theta_{i1}=(i-1)\frac{\pi}{2}+\frac{\beta}{2}-\phi_B$, and β is half of the distribution angle of static pressure region. Substituting $\theta=\theta_{i2}=i\frac{\pi}{2}-\frac{\beta}{2}-\phi_B$ into Eq.(6) yields the coefficient C_1 expression as follows

$$C_1=\frac{p_{c,i+1}-p_{c,i}-\frac{6\mu R^2\dot{\varepsilon}}{C^2\varepsilon}C_2}{\int_{\theta_{i1}}^{\theta_{i2}}\frac{1}{C^3(1+\varepsilon\cos\theta)^3}d\theta},\ C_3=\int_{\theta_{i1}}^{\theta_{i2}}\frac{12\phi_B\mu C\varepsilon R^2\cos\theta}{C^3(1+\varepsilon\cos\theta)^3}d\theta,$$

$$C_2=\frac{1}{(1+\varepsilon\cos\theta_{i2})^2}-\frac{1}{(1+\varepsilon\cos\theta_{i1})^2}+C_3.$$

In area of HSFD with $a\leqslant|z|\leqslant L/2$, the pressure distribution can be solved as follows

$$p(z,\theta)=(\frac{L}{2}-|z|)\Big[[A_1(\theta)\dot{\phi}_B\varepsilon+A_2(\theta)\dot{\varepsilon}](a-|z|)+p_0(\theta)\Big/(\frac{L}{2}-a)\Big] \tag{7}$$

where $A_1(\theta)=\frac{6\mu C\sin\theta}{C^3(1+\varepsilon\cos\theta)^3}$, $A_2(\theta)=\frac{6\mu C\cos\theta}{C^3(1+\varepsilon\cos\theta)^3}$.

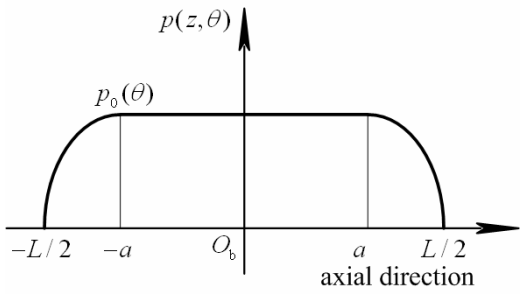

Figure 2. Pressure distribution of axial direction in HSFD

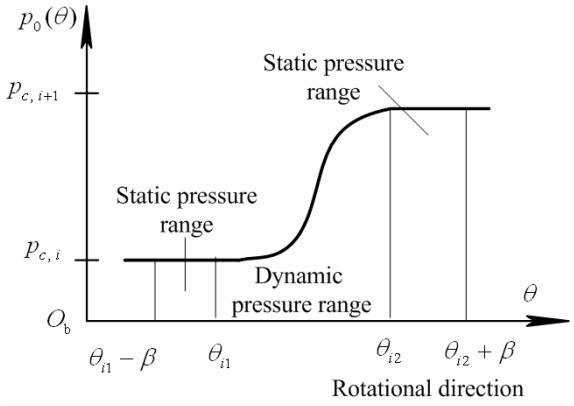

Figure 3. Pressure distribution of rotational direction in HSFD

B. Solution of the instant oil film supporting force

The oil film forces of HSFD oil pressure can be determined when the oil film pressure of static pressure region decided by Renault equations is achieved. The oil film force of HSFD consists of 3 parts: static pressure oil film forces, axis direction dynamic pressure region forces and the rotational direction dynamics pressure region forces. The force components in the area of static pressure region and the dynamic pressure region can be respectively given as follows

$$\begin{cases} F_{sr}=2aR\sum_{i=1}^{4}(\sin\theta_{i1}-\sin(\theta_{i1}-\beta-\phi_B))p_{c,i} \\ F_{st}=2aR\sum_{i=1}^{4}(\cos\theta_{i1}-\cos(\theta_{i1}-\beta-\phi_B))p_{c,i} \end{cases} \tag{8}$$

$$\begin{cases} F_{tr}=\sum_{i=1}^{4}\int_{\theta_{i1}}^{\theta_{i2}}p_i(\theta)\cdot 2aR\cos\theta d\theta \\ F_{tt}=\sum_{i=1}^{4}\int_{\theta_{i1}}^{\theta_{i2}}p_i(\theta)\cdot 2aR\sin\theta d\theta \end{cases} \tag{9}$$

where $p_i(\theta)$ can be determined by Eq.(6). In the area of $a\le|z|\le L/2$ at axis direction, with the symmetry character, the oil film forces supplied by the oil film pressure forces can be determined by the equations as follows

$$\begin{cases} F_{ar}=2\int_a^{L/2}dz\int_0^{2\pi}p(z,\theta)R\cos\theta d\theta \\ F_{at}=2\int_a^{L/2}dz\int_0^{2\pi}p(z,\theta)R\sin\theta d\theta \end{cases} \tag{10}$$

Based on the above-analyzed results, the total oil film forces can be solved as $F_r=F_{sr}+F_{tr}+F_{ar}$, and $F_t=F_{st}+F_{tt}+F_{at}$.

C. Rotor Dynamics Equation

The force diagram of rotor support system shows in Fig.4, O_b is center of oil film ring, O_j is oil film journal center, O_c is gravity center. The load can be got through the motion and force analysis: unbalanced exciting force caused by mass eccentricity, centrifugal inertia force brought by motion, oil film force and elastic restore force of bearing, and inertia force in journal center created by precession acceleration that around the oil film ring.

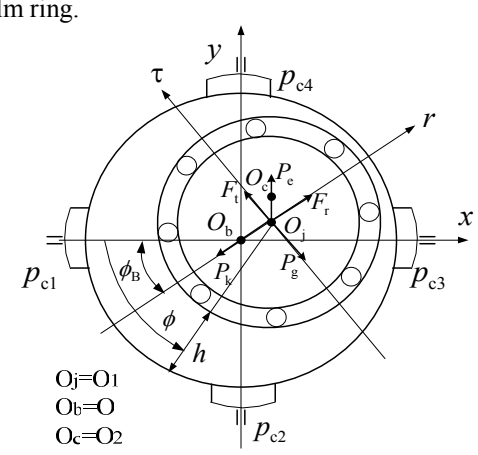

Figure 4. Force analysis of a rotor with HSFD

Assuming that the rotor speed is ω_s, v is mass relative eccentricity, $e_m=U_c$ is mass eccentricity, m is the rotor mass that lumped at the mid-point. By using free-body method to carry out the analysis to the action forces applied to rotor-supporting system, the dynamical model is described as follows

$$\begin{cases} \ddot{\varepsilon}-\varepsilon\dot{\phi}_B^2=h_1+v\cos(\omega_s t-\phi_B)-h_2\varepsilon-2\xi\dot{\varepsilon}/\omega \\ \varepsilon\ddot{\phi}_B+2\dot{\varepsilon}\dot{\phi}_B=h_3+v\sin(\omega_s t-\phi_B)-2\xi\dot{\varepsilon}\dot{\phi}_B/\omega \end{cases} \tag{11}$$

where $\omega=\frac{\omega_s}{\omega_c}$, $h_1=\frac{F_r}{mC\omega_s^2}$, $h_2=\frac{K}{mC\omega_s^2}$, $h_3=F_t/(mC\omega_s^2)$.

Combining Eq.(11) with Eq.(2) to Eq.(10), yields the mathematical model of the overall HSFD system.

III. DYNAMIC DIGITAL SIMULATION OF HSFD

A. Procedure of the digital simulation

Fig.5 shows the whole computing simulation process of HSFD dynamic characteristics. In the start of first calculation, a set of initial values $\varepsilon_0, \dot{\varepsilon}_0, \phi_{B0}, \dot{\phi}_{B0}$ are taken into PD control Eq.(4) to confirm the initial pressure $p_{c,i}$ in static pressure chamber, and then the oil film pressures of every position can be solved through taking $p_{c,i}$ into Eq.(5) and Eq.(7). With that the oil film forces in static pressure chamber, rotational pressure range and axial pressure range are achieved in Eq.(8-10). Afterward, taking the above three forces into Eq.(11) and the $\varepsilon, \dot{\varepsilon}, \phi_B, \dot{\phi}_B$ could be got by solving second-order differential equations with Runge-Kutta method, then a new turn iteration process is started by taking the first solutions of $\varepsilon, \dot{\varepsilon}, \phi_B, \dot{\phi}_B$ into Eq.(4).

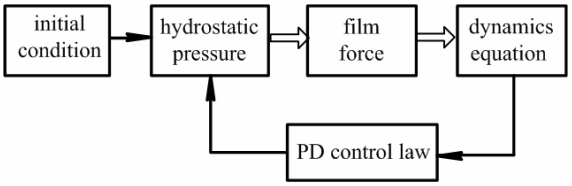

Figure 5. Calculating procedure diagram

The main parameters are as follows: damping ratio $\xi = 0.0005$, oil chamber numbers n=4, critical speed $\omega_c = 140\pi$ rad/s, oil density $\rho = 850$ kg/m^3, $\mu = 0.008$ m^2/s, a=0.012m, L=0.04m, R=0.03m, $p_s = 1\times10^6$ Pa, C=5.3$\times10^{-4}$ m.

Runge-Kutta algorithm is used to solve the dynamics equations. On step division, the computing experience in reference [3] will be consulted, that means 540 points will be picked out in rotor one cycle rotation and the instant data of the first cycles are abandoned in order to ensure steady state motion can be arrived.

Define abbreviations and acronyms the first time they are used in the text, even after they have been defined in the abstract. Abbreviations such as IEEE, SI, MKS, CGS, sc, dc, and rms do not have to be defined. Do not use abbreviations in the title or heads unless they are unavoidable.

B. Parameter working scale discussion of HSFD active control program

The computing results above show the bifurcation and chaos dynamics characteristics as the rotating speed ratio ω is variation in the condition that the proportional control coefficient k_p is fixed; besides, the same characteristics are existed when ω is fixed and k_p is variation. So it is proved that the period-doubling and chaos motion can be completely eliminated to make the trace of rotor axial center always keep the state of limit loop as long as properly regulating coefficient k_p, when in the condition of fixed rotating speed. It is very significant to enhance rotor speed and increase the fatigue lifespan.

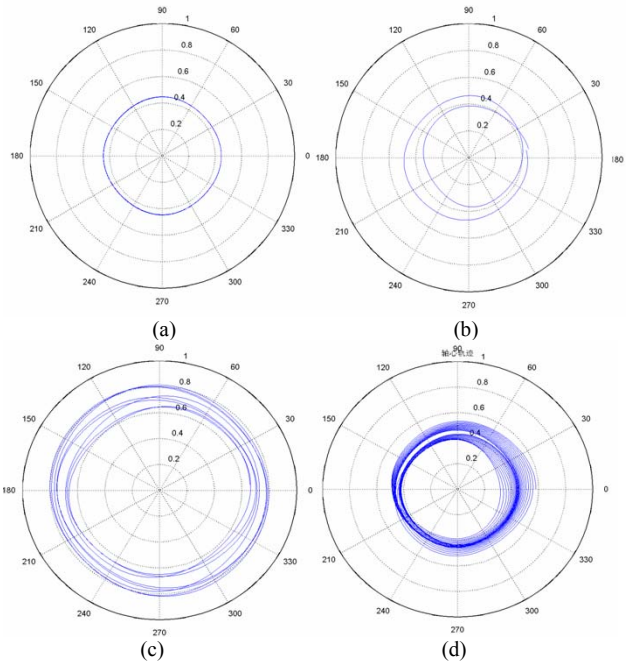

Figure 6. Relationship between the solution types and parameter k_p

The whole computing process adopts MATLAB language program and divides rotor's one rotation cycle into 540 steps to calculate. Taking ω=1.2 for example, the simulation will choose the initial value ε_0 =0.6(X=0.6, Y=0) according to assumption of coordination circle precession, then to observe the solution through regulating the proportional control coefficient k_p. Fig.6 (a)-(d) are the motion traces of rotor axial center in condition of the k_p values to be 1.1,1.6,1.7,1.74 respectively. There into, Fig.6(b) and (c) are trajectories of 2-period solution and 4-period solution separately, and there may exists chaos solutions when on some ω values and k_p is in certain scale (e.g. k_p=1.74). So it means that keeping the rotor dynamics states always be 1-period solution as long as choosing proper k_p value scale in appropriate rotating speeds. For every ω value, a corresponding k_p interval which makes the rotor stay in the state of 1-period solution can be obtained, and Fig.7 shows the diagram. Rotor only stays in the state of 1-period solution no matter which speed rotor has, when k_p adopts values in the shadow area.

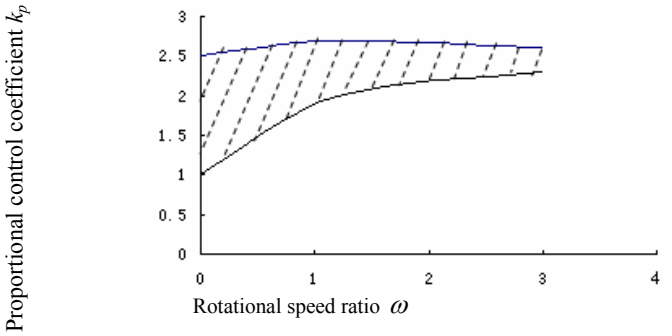

Figure 7. Proportional gain kp versus Rotational speed ratio ω when the axis centre trajectory keeps 1-preiod solution

In the implementation process, rotor rotating speed ratio is easily measured by speed sensor; and it is convenient to adjust the proportional coefficient of PD controller for the computer control system. This procedure is actually to determine a series of $\omega \rightarrow k_p$ maps. If $\omega \rightarrow k_p$ map is known, the active control of high speed rotor can be implemented in the condition of choosing proper coefficient k_p according to the measured rotating speed ratio ω.

IV. CONCLUSIONS

In the paper, it is studied that rotor supporting system of squeeze-film damper with active control has two motion states of bifurcation and chaos by using the digital simulation for HSFD system. The complicated bifurcation and chaos dynamics characteristics of HSFD system have been analyzed by the quantitative and qualitative methods from the diagrams of phase traces and bifurcation charts.

Furthermore, it is found that HSFD system also shows the bifurcation and chaos dynamics states in some fixed speed, as the proportional coefficient k_p variation. So the motions of 2-period and chaos in system can be eliminated and to make HSFD system stay in 1-period state, as long as choosing the proper proportional differential controller. Based on this, an active control idea for high speed rotor in HSFD system was put forward. It is significant to increase rotor working speed and fatigue lifespan and decrease body vibration.

REFERENCES

[1] C.-L. Chen, H.-T. Yau and Y.-H. Li, "Sub-harmonic and Chaotic Motions of a Hybrid Squeeze-Film Damper-Mounted Rigid Rotor With Active Control," ASME J. Vibration and Acoustics, vol.124, no.2, pp. 198-208, Apr., 2002

[2] S. Wingins, "Introduction to Applied Nonlinear Dynamical Systems and Chaos," Springer-Velag, World Publishing Corp, 1990

[3] H.E. Merritt, "Hydraulic Control Systems," New York:Wiley, 1967

[4] Litang Yan, "Analysis on Dynamic Characteristics of Structure Systems(In Chinese)", Beijing: Beijing University of Aeronautics and Astronautics Press, 1989

[5] Y.-H. Li, Zhanlin Wang, Chieh-Li Chen, "Solution for Pressure Distribution in Squeeze Film Damper with Electro-hydraulic Active Control," Chinese J.of Mech. Engrs., vol.12, no.1, pp27-31, Feb., 1999

[6] X.-C. Gao and Y.-H. Li, "Active Control Research for the Rotor System Vibration Based on the Electro-hydraulic Controllable Squeeze Film Damper," Machine Tool & Hydraulics, no.5, pp11-13, Dec., 2002

[7] C.-S. Zhu, "Periodic Bifurcation Behaviors of the Flexible Rotor System with Non linear Squeeze Film Damper," Journal of Vibration Engineering, vol.10, no.3, pp333-349, June, 1997

[8] J.-Y. Zhao and E.-J. Hahn, "Sub-harmonic, quais-periodic and chaotic motions of a rigid rotor supported by an eccentric squeeze film damper," J. of Mech. Engrs., vol. C207, no.3, pp383-392, June, 1993

[9] Litang Yan, "Vibration of Rotational Machine with High Speed," Beijing: China National Defense Industry Press, 1994